ELSEVIER

Life Sciences 69 (2001) 2503–2515

Life Sciences

Advanced glycosylation end products induce nitric oxide synthase expression in C6 glioma cells Involvement of a p38 MAP kinase-dependent mechanism

Chien-Huang Lin[a], Yuan-Fong Lin[b], Meng-Chu Chang[a], Chih-Hsiung Wu[c], Yuan-Soon Ho[a], Horng-Mo Lee[a,*]

[a]*Graduate Institute of Biomedical Technology, Taipei Medical University, Taipei, Taiwan, R.O.C.*
[b]*Pharmaceutical Sciences, Taipei Medical University, Taipei, Taiwan, R.O.C.*
[c]*School of Medicine, Taipei Medical University, Taipei, Taiwan, R.O.C.*

Received 1 December 2000; accepted 25 April 2001

Abstract

The mitogen-activated protein kinase (MAPK) pathway is believed to function as an important mediator of inducible nitric oxide synthase (iNOS) expression. In the present study, we investigated the role of the p38 MAPK signaling pathway in advanced glycosylation end products (AGEs)-induced iNOS expression in C6 glioma cells. AGEs caused a dose-dependent increase of nitrite accumulation in C6 glioma cells. The AGEs-stimulated nitrite production from C6 glioma cells was inhibited by actinomycin D, cyclohexamide, and the NO synthase inhibitor, N_{ω}-nitro-$_{L}$-arginine methyl ester (L-NAME), suggesting that the increase of AGEs-induced nitrite release is due to iNOS up-regulation. Consistently, treatment of C6 glioma cells with AGEs induced iNOS protein expression. AGEs-stimulated nitrite production was inhibited by pretreatment of C6 glioma cells with anti-AGEs antibodies (1:100 or 1:50). The tyrosine kinase inhibitor (genistein and tyrphostin), the Ras-farnesyl transferase inhibitor (FPT inhibitor-II), or the p38 MAPK inhibitor (SB203580) suppressed AGEs-induced iNOS expression and nitrite release from C6 glioma cells. AGEs activated p38 MAPK in C6 glioma cells, and this effect was blocked by genistein (20 μM), tyrphostin (30 μM), FPT inhibitor-II (20 μM), and SB203580 (10 μM). Taken together, our data suggest that AGEs may activate the pathways of tyrosine kinase and Ras to induce p38 MAPK activation, which in turn induces iNOS expression and NO production in C6 glioma cells. © 2001 Elsevier Science Inc. All rights reserved.

Keywords: AGEs; iNOS; C6 glioma cells; p38 MAPK

* Corresponding author. Graduate Institute of Biomedical Technology, Taipei Medical University, 250 Wu-Hsing Street, Taipei 110, Taiwan. Fax: 886-2-2732-4510.

E-mail address: leehorng@tmu.edu.tw (H-M. Lee)

0024-3205/01/$ – see front matter © 2001 Elsevier Science Inc. All rights reserved.
PII: S0024-3205(01)01330-3

Introduction

Advanced glycosylation end products (AGEs) are fluorescent substances formed by the non-enzymatic "Maillard reaction" [1]. Several lines of evidence indicate that AGEs contribute to the pathogeneses of diabetic complications and aging [2]. Accumulation of AGEs in the brain is the biochemical basis of Alzheimer's disease including extensive protein cross-linking [3, 4]. The toxic actions of advanced glycosylation end products have also been demonstrated in gingiva [5], in the human penis [6], in cultured retinal capillary pericytes and endothelial cells [7], in mature human monocytes and human monocytic THP-1 cells [8], and in murine macrophages [9, 10].

Nitric oxide (NO) is a diffusible gas that is generated enzymatically from L-arginine and molecular oxygen by nitric oxide synthase (NOS). To date, at least three different types of NOS have been characterized. The endothelial type (eNOS) and the neuronal type (cNOS) are constitutively expressed, whereas the inducible type (iNOS) is induced by a variety of signals in many cell types [11]. NO plays important roles in both physiological and pathological conditions. Low concentrations of NO have been shown to serve as a neurotransmitter and a vasodilator, while at high concentrations it is toxic and may be important in several neurodegenerative diseases [12]. Overproduction of NO in the brain is the biochemical basis of many neuropathological features, such as oxidative stress [13] and neuronal cell death [14, 15]. Microglial cell-derived NO can contribute to oligodendrocyte degeneration and neuronal cell death. In Alzheimer's disease, neurons are subjected to the deleterious cytotoxic effects of activated microglia [4]. However, the roles of AGEs-induced NO production in Alzheimer's disease have not been effectively addressed.

AGEs induce iNOS expression in a variety of cell lines [9, 16]. AGEs regulate many cell functions through AGEs-specific receptors, RAGEs [17, 18]. Activation of the RAGEs may trigger the p21 (Ras)-dependent mitogen-activated protein kinase (MAPK) pathway in many cell types [19, 20]. Thus, the Ras-MAPK pathway may be the upstream signal that contributes to AGEs-induced iNOS expression. Presently, three parallel protein phosphorylation cascades in mammalian cells have been described.

In the present study, the mechanism of the signal transduction cascade involved in the induction of iNOS in response to AGEs was studied. Our data revealed that AGEs may activate the pathways of tyrosine kinase and Ras to induce p38 MAPK activation, which in turn results in iNOS induction and, finally, NO release from C6 glioma cells.

Methods

Materials

Dobellco's modified Eagle's medium (DMEM), fetal calf serum (FCS), glutamine, gentamycin, penicillin, and streptomycin were purchased from Life Technologies (Gaithersburg, MD). Antibodies specific for iNOS and α-tubulin were purchased from Santa Cruz Biochemicals (Santz Cruz, CA). Actinomycin D, cyclohexamide, N_{ω}-nitro-$_{L}$-arginine methyl ester (L-NAME), SB203580, genistein, and FPT inhibitor-II were purchased from Calbiochem-Novabiochem (San Diego, CA). HRP-conjugated anti-rabbit IgG antibody was purchased from Bio Rad

(Hercules, CA). p38 MAPK activity assay kit was purchased from New England Biolabs, Inc (Beverly, MA). All other chemicals were purchased from Sigma (St Louis, MO).

Preparation of albumin-derived advanced glycosylation end products

Bovine serum albumin (BSA)-derived AGEs were prepared by incubating 1 M glucose with 50 mg/ml BSA in phosphate buffered saline (PBS), pH 7.4, for at least 6 months. All incubations were performed under sterile conditions in the dark at 37 °C. After incubation, unreacted sugars were removed before assay by extensive dialysis against PBS. The BSA-AGEs solution was filter-sterilized and stored in a freezer before use.

Preparation of polyclonal anti-AGEs antibodies

BSA-AGEs (1.0 mg) were emulsified in 50% complete Freund adjuvant (1 ml) and were injected intradermally into New Zealand White rabbits at 6–10 skin sites. Ten days after the primary injection, rabbits were boosted with the same amount of BSA-AGEs emulsified in 50% complete Freund adjuvant. The same antigen preparations were used for four-booster injections every week. The final boost was given by injecting 2.0 mg of BSA-AGEs emulsified in 50% incomplete Freund's adjuvant intradermally and intramuscularly 2 weeks after the last injection. Venous puncture was performed to collect blood 10 days after the final booster injection. Serum was pooled, fractionated with ammonium sulfate, and immunoabsorbed with 50 mg/ml of BSA. Direct ELISA was used to determine the immunoreactivity and specificity of the rabbit anti-AGEs antibodies.

Culture of C6 glioma cells and preparation of cell lysates

C6 glioma cells were cultured in DMEM supplemented with 13.1 mM $NaHCO_3$, 13 mM glucose, 2 mM glutamine, 10% heat-inactivated FCS, and penicillin (100 U/ml)/ streptomycin (100 mg/ml). Cells were attached to a petri dish after a 24h incubation. Cells were plated at a concentration of 1×10^5 cells/ml and used for the experiment when they reached 80% confluency. Cultures were maintained in a humidified incubator in 5% CO_2 at 37 °C. After reaching confluence, cells were treated with various concentrations of BSA-AGEs for 24 h or 300 μg/ml BSA-AGEs for indicated time intervals and incubated in a humidified incubator at 37 °C. In some experiments, cells were treated with vehicle, BSA-AGEs (300 μg/ml), or pretreatment with specific inhibitors as indicated followed by BSA-AGEs and incubated in a humidified incubator at 37 °C. After incubation, cells were lysed by adding lysis buffer containing 10 mM Tris HCl, pH 7.5, 1 mM EGTA, 1 mM $MgCl_2$, 1 mM sodium orthovanadate, 1 mM DTT, 0.1% mercaptoethanol, 0.5% Triton X-100, and the protease inhibitor cocktails (final concentrations: 0.2 mM PMSF, 0.1% aprotinin, 50 μg/ml leupeptin). Cells adhering to the plates were scraped off using a rubber policeman and stored at −70 °C for further measurements.

Polyacrylamide gel electrophoresis and Western blotting

Electrophoresis was ordinarily carried out by different percentages of SDS-polyacrylamide electrophoresis (SDS-PAGE). Following electrophoresis, proteins on the gel were electrotransferred onto a nitrocellulose or polyvinyldifluoride (PVDF) membrane. After transfer, the PVDF membrane was washed once with PBS and twice with PBS plus 0.1% Tween 20.

The PVDF membrane was then blocked with blocking solution containing 3% bovine serum albumin in PBS containing 0.1% Tween 20 for 1 h at room temperature. The PVDF membrane was incubated with a solution containing primary antibodies in the blocking buffer. Finally, the PVDF membrane was incubated with peroxidase-linked anti-mouse IgG antibodies for 1 h and then developed using a commercially available chemiluminescence kit (Amersham, UK).

Measurement of nitrite formation in C6 glioma cultures

C6 glioma cells were cultured in 35-mm petri dishes. After reaching confluence, cells were treated with various concentrations of BSA-AGEs for 24 h or 300 μg/ml BSA-AGEs for indicated time intervals and incubated in a humidified incubator at 37 °C. In some experiments, cells were treated with vehicle, BSA-AGEs (300 μg/ml), or pretreatment with specific inhibitors as indicated followed by BSA-AGEs and incubated in a humidified incubator at 37 °C. After incubation, the medium was removed and stored at −80 °C until assay of nitrite accumulation. Nitrite production was measured by adding 0.15 ml of the cell culture medium to 0.15 ml of Griess reagent [21] in a 96-well plate, and incubated in a dark place at 37 °C for 10 min. Absorbance was measured at 540 nm using a microplate reader. A blank was prepared for each experimental condition in the absence of C6 glioma cells, and the absorbance was subtracted from that obtained in the presence of cells.

Measurement of p38 MAPK activity

The activity of p38 MAPK was measured by using p38 MAPK activity assay kit (New England Biolabs, Inc). Briefly, C6 glioma cells were cultured in 10-cm petri dishes. After reaching confluence, cells were treated with 300 μg/ml BSA-AGEs for indicated time intervals and incubated in a humidified incubator at 37 °C. In some experiments, cells were treated with vehicle, BSA-AGEs (300 μg/ml), or pretreatment with specific inhibitors as indicated followed by BSA-AGEs and incubated in a humidified incubator at 37 °C. After incubation, cells were washed with phosphate buffer saline (PBS, pH 7.4). Proteins were extracted with lysis buffer (Tris 20 mM; pH 7.5; NaCl 150 mM; EDTA 1 mM, EGTA 1 mM, Triton 1%, sodium pyrophosphate 2.5 mM, β-glycerolphosphate 1 mM, Na_3VO_4 1 mM, leupeptin 1 μg/ml) with gentle shaking, centrifuged, mixed 1:1 with sample buffer (Tris 100 mM, pH 6.8; 20% glycerol; 4% SDS and 0.2% Bromophenol Blue), and then boiled for 5 min. Cell extracts were incubated with anti-phospho-p38 MAPK antibody, which was immobilized to crosslinked agarosed hydrazide beads, for overnight at 4°C. The beads were then centrifuged for 30 sec at 4°C. The cell pellet was washed twice with lysis buffer, and then incubated with 50 μl of kinase buffer (Tris 25 mM, pH 7.5, β-glycerolphosphate 5 mM, DTT 2 mM, Na_3VO_4 0.1 mM, and $MgCl_2$ 10 mM) supplemented with 200 μM of ATP and 2 μg of ATF-2 for 60 min at 30 °C. The reaction was terminated by the addition of 3× SDS sample buffer and subjected to 10% SDS-PAGE gel. The phosphorylated ATF-2 was detected using Lumi-GLO chemiluminescent reagent, and exposed to X-ray film.

Statistical analysis

Results are expressed as means±s.e.mean. from 3–4 independent experiments. One-way analysis of variance (ANOVA) followed by, when appropriate, Bonferroni multiple range test

was used to determine the statistical significance in the difference between means. A *P*-value of less than 0.05 was taken as statistically significant.

Results

AGEs stimulated a dose-dependent increase in NO release

AGEs stimulated nitrite production from C6 glioma cells in dose- (Fig. 1A) and time-dependent manners (Fig. 2A). The EC_{50} of AGEs-stimulated nitrite accumulation was about

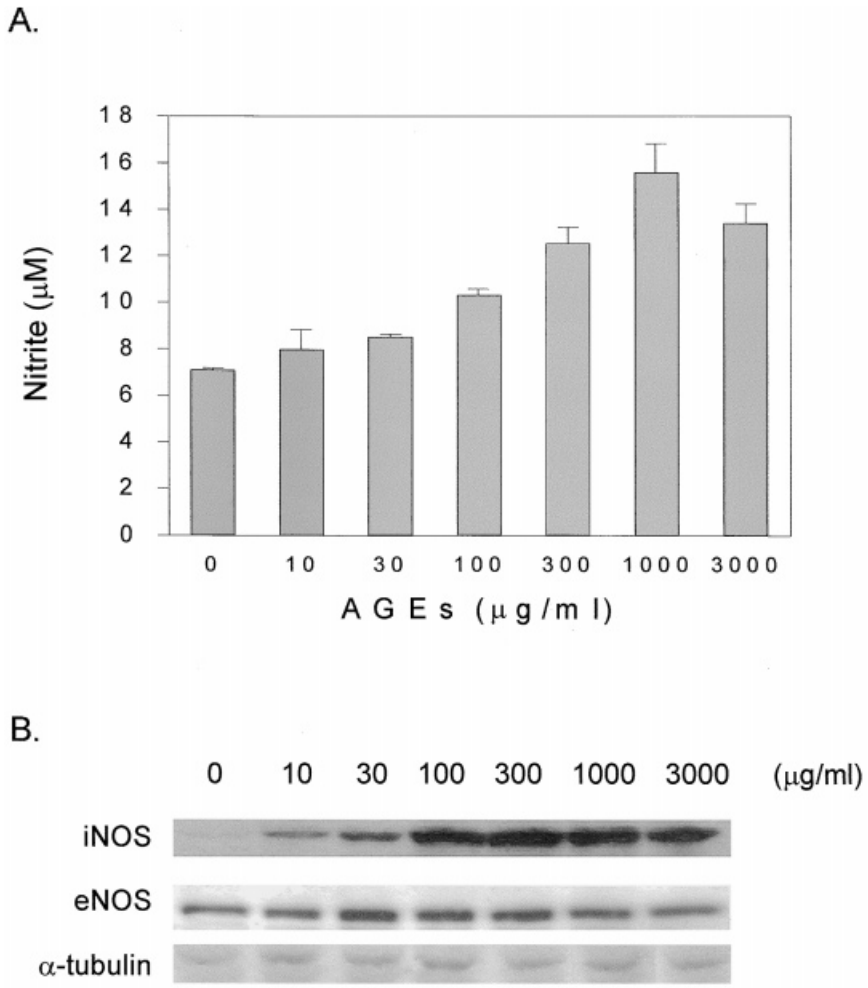

Fig. 1. Dose-dependent increase of nitrite accumulation and iNOS expression caused by BSA-AGEs in C6 glioma cells. Cells were incubated with various concentrations of BSA-AGEs for 24 h, then the medium was removed and analyzed for nitrite accumulation (A). Data represent the mean ± S.E.M. of three independent experiments in triplicate. In (B), cells were incubated with various concentrations of BSA-AGEs for 24 h, and then immunodetected with iNOS or eNOS specific antibody as described in *Methods.* Equal loading in each lane was demonstrated by the similar intensities of α-tubulin.

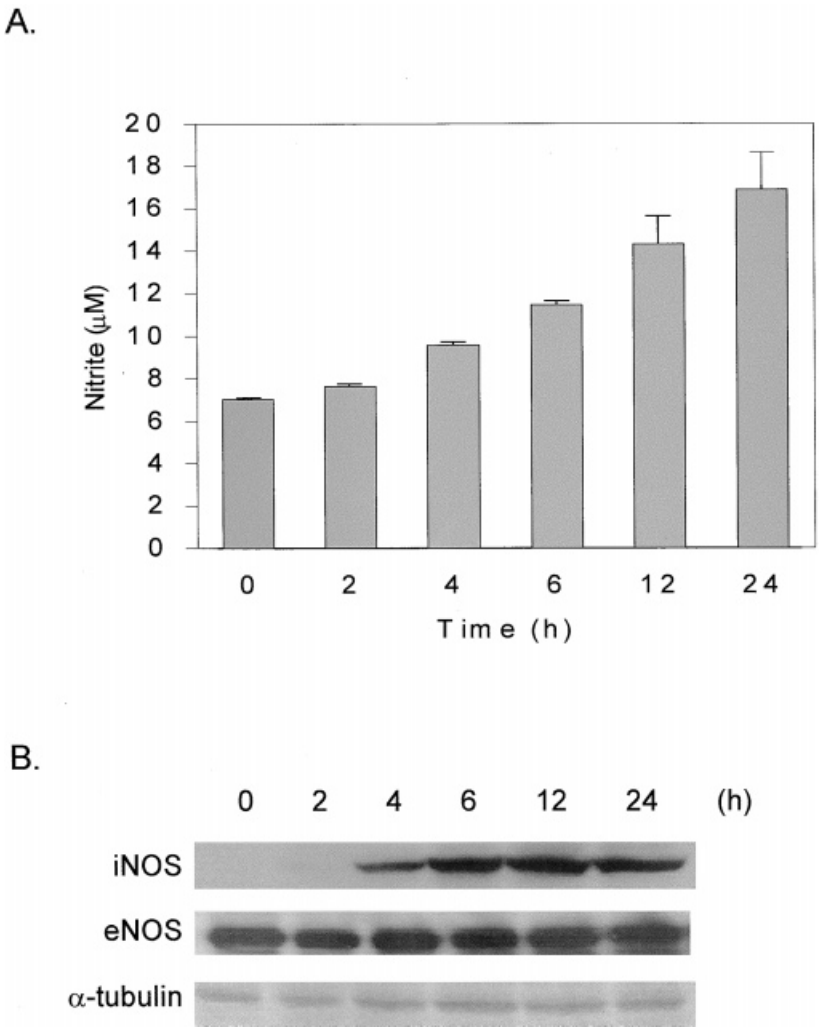

Fig. 2. Time-dependent increase of nitrite accumulation and iNOS expression caused by BSA-AGEs in C6 glioma cells. Cells were incubated with 300 μg/ml BSA-AGEs for various time periods, then the medium was removed and analyzed for nitrite accumulation (A). Data represent the mean ± S.E.M. of three independent experiments in triplicate. In (B), cells were incubated with 300 μg/ml BSA-AGEs for various time periods, and then immunodetected with iNOS or eNOS specific antibody as described in *Methods.* Equal loading in each lane was demonstrated by the similar intensities of α-tubulin.

100 μg/ml, with the maximum at 1000 μg/ml of AGEs after 24 h of treatment. The AGEs-stimulated nitrite release was apparent after 6 h of treatment and accumulated thereafter. Consistently, AGEs induced the expression of 130-kDa iNOS but not the constitutively expressed eNOS in C6 glioma cells (Fig. 1B and 2B). The induction became apparent at 6 h with the maximum at about 24 h (Fig. 2B). When cells were pretreated for 30 min with the anti-AGEs antibody (1:50 or 1:100), L-NAME (1 mM), actinomycin D (1 μM), or cycloheximide (10 μM), the AGEs-induced nitrite release was blocked by anti-AGEs antibody,

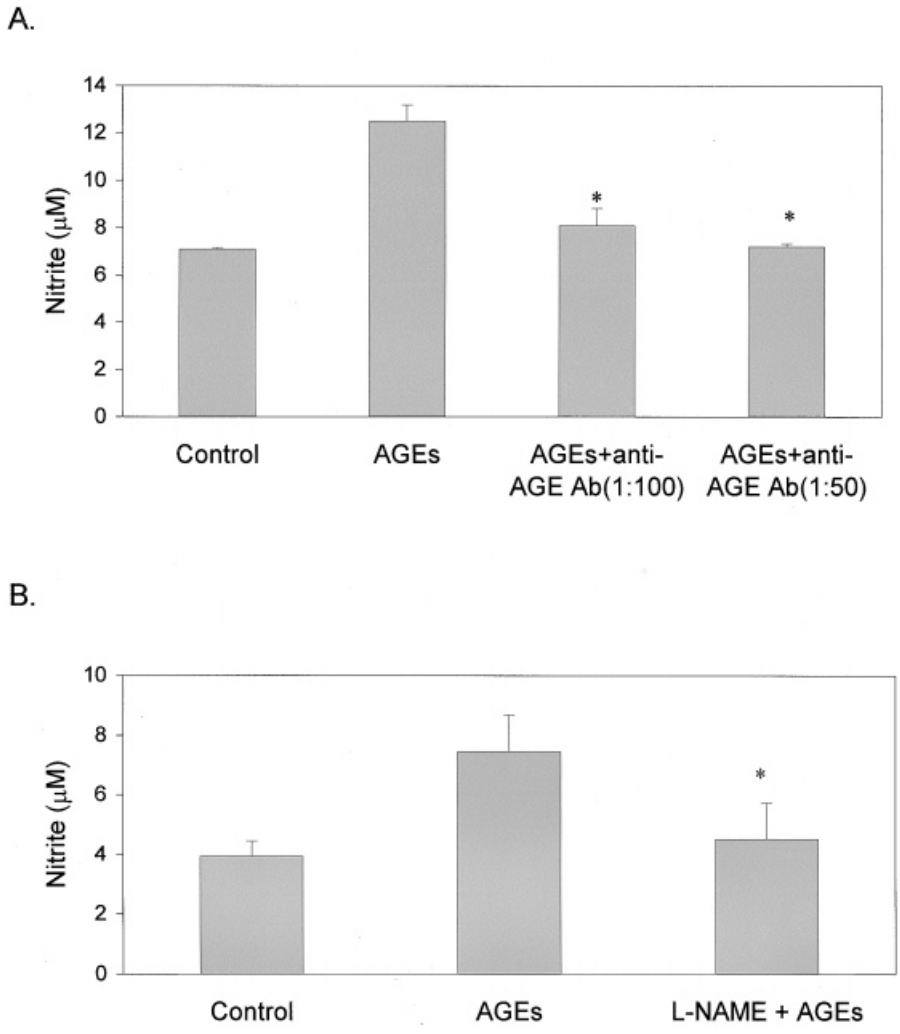

Fig. 3. Effects of anti-AGEs antibody (A) and L-NAME (B) on AGEs-induced nitrite production in C6 glioma cells. C6 glioma cells were pretreated with anti-AGEs antibody (1:50 or 1:100) or L-NAME (1 mM) for 30 min before the addition of 300 μg/ml BSA-AGEs for 24 h. Then the medium was removed and analyzed for nitrite accumulation. C6 glioma cells were pretreated with 300 μg/ml BSA-AGEs in the absence or presence of, and the medium was removed and analyzed for nitrite accumulation. Data represent the mean ± S.E.M. of three independent experiments in triplicate. * $P<0.05$ as compared with the AGEs-treated group.

L-NAME, actinomycin D, and cyclohexamide (Fig 3, 4). The results suggest that AGEs-specific transcription and de novo protein synthesis are required.

Involvement of Ras-MAPK signaling pathway in AGEs-stimulated iNOS expression and nitrite production by C6 glioma cells

Activation of the receptors of AGEs (RAGE) may trigger a p21 Ras-MAPK-related signal transduction cascade [19]. We next investigated the effects of a tyrosine kinase inhibitor

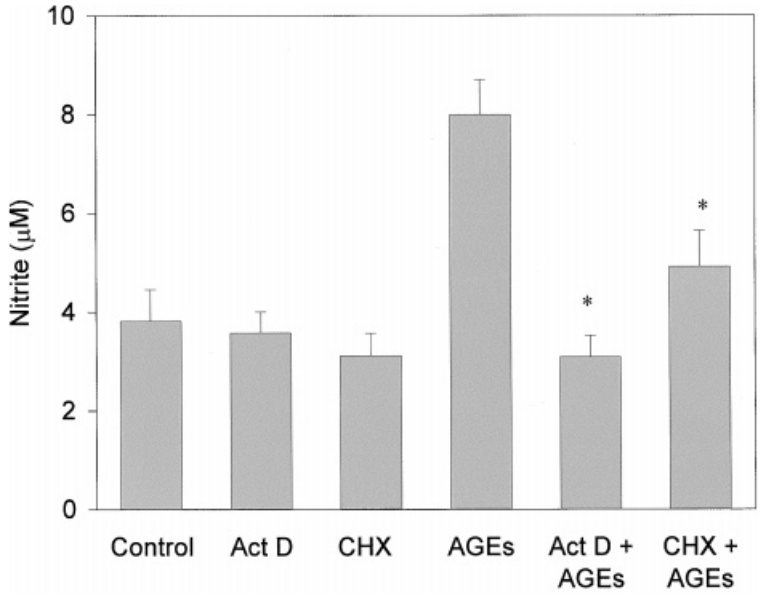

Fig. 4. Effects of actinomycin D and cyclohexamide on AGEs-induced nitrite production in C6 glioma cells. C6 glioma cells were pretreated with actinomycin D (Act D, 1 μM) or cyclohexamide (CHX, 10 μM) for 30 min before the addition of 300 μg/ml BSA-AGEs for 24 h. Then the medium was removed and analyzed for nitrite accumulation. Data represent the mean ± S.E.M. of three independent experiments in triplicate. *$P<0.05$ as compared with the AGEs-treated group.

(genistein and tyrphostin), a Ras-farnesyl transferase inhibitor (FPT inhibitor-II), and a p38 MAPK inhibitor (SB203580) on AGEs-stimulated nitrite accumulation. Fig. 5 shows that genistein (20 μM), FPT inhibitor-II (20 μM), SB203580 (10 μM), and tyrphostin (30 μM) all attenuated AGEs-stimulated nitrite release and iNOS expression. Thus, the activations of tyrosine kinase, Ras, and p38 MAPK seem to be involved in the AGEs-mediated signal transduction leading to the iNOS expression and NO release.

Activation of p38 MAPK by BSA-AGEs in C6 glioma cells

The data in Fig. 5 suggest that the p38 MAPK-activated pathway might contribute to the signaling mechanism for AGEs-induced iNOS expression in C6 glioma cells. This notion was supported by the fact that AGEs activate p38 MAPK in C6 glioma cells. As shown in Fig. 6, addition of BSA-AGEs to C6 glioma cells stimulated the increase in p38 MAPK activity as determined with an immunocomplex kinase assay using ATF-2 as the substrate. p38 MAPK was transiently activated within 15 min, reached a maximum at about 1 h, and then decreased by 3 h. Western blot analysis using anti-p38 MAPK antibodies indicated that the total protein expression of p38 MAPK was unaffected by BSA-AGEs induction. When cells were pretreated for 30 min with SB203580 (10 μM), genistein (20 μM) or FPT inhibitor-II (20 μM), the BSA-AGEs-induced activation of p38 MAPK was markedly inhibited by SB203580, genistein, and FPT inhibitor-II (Fig. 7).

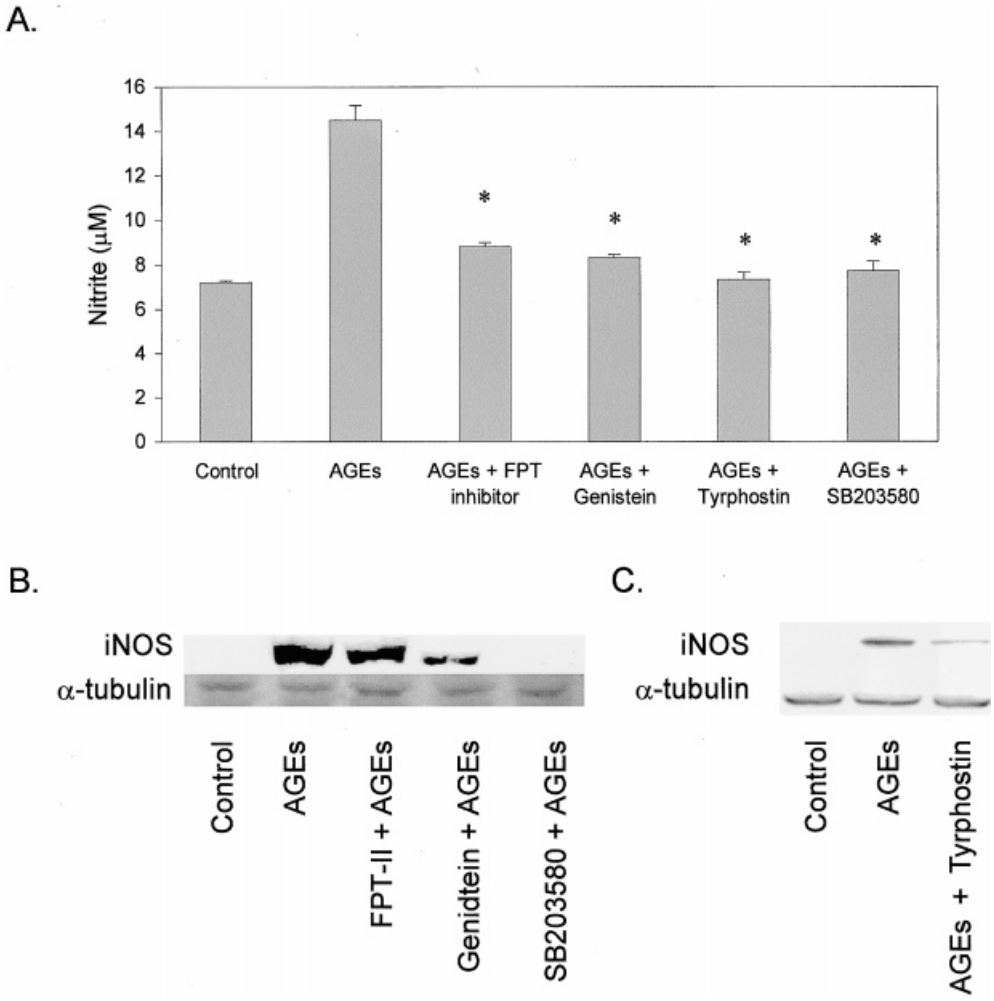

Fig. 5. Effects of FPT inhibitor-II, genistein, SB203580, and typhorstin on AGEs-induced nitrite production and iNOS expression in C6 glioma cells. In (A), cells were pretreated with FPT inhibitor-II (20 μM), genistein (20 μM), SB203580 (10 μM), or typhorstin (30 μM) for 30 min before the addition of 300 μg/ml BSA-AGEs for 24 h. Then the medium was removed and analyzed for nitrite accumulation. Data represent the mean ±S.E.M. of three independent experiments in triplicate. * $P<0.05$ as compared with the AGEs-treated group. In (B) and (C), cells were pretreated with FPT inhibitor-II (20 μM), genistein (20 μM), SB203580 (10 μM), or typhorstin (30 μM) for 30 min prior to a 24 h incubation with 300 μg/ml BSA-AGEs. The cells were then prepared for immunodetection using iNOS specific antibody as described in *Methods.* Equal loading in each lane was demonstrated by the similar intensities of α-tubulin.

Discussion

In the present study, we demonstrate that AGEs increase nitrite production and iNOS expression in C6 glioma cells. Given that iNOS upregulation was observed in astrocytes surrounding amyloid plagues [22] and peroxynitrite damage to neurons has been observed in the brain of Alzheimer's disease [23]. The iNOS induction may play an important role in the

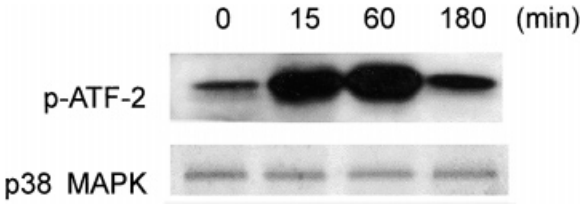

Fig. 6. AGEs activate p38 MAPK in C6 glioma cells. Cells were incubated with 300 μg/ml BSA-AGEs for various time periods, cells were lysed, and the p38 MAPK activity was determined by immunocomplex kinase assay using ATF-2 as the substrate as described in *Methods.* Equal loading in each lane was demonstrated by a similar protein level of p38 MAPK.

pathogeneses of Alzheimer's disease. In this study, we present evidence that AGEs-stimulated iNOS expression is mediated through the pathways of tyrosine kinase, Ras and p38 MAPK. Understanding the signal transduction pathway that ultimately leads to deleterious effects in the central nervous system is important from a therapeutic standpoint.

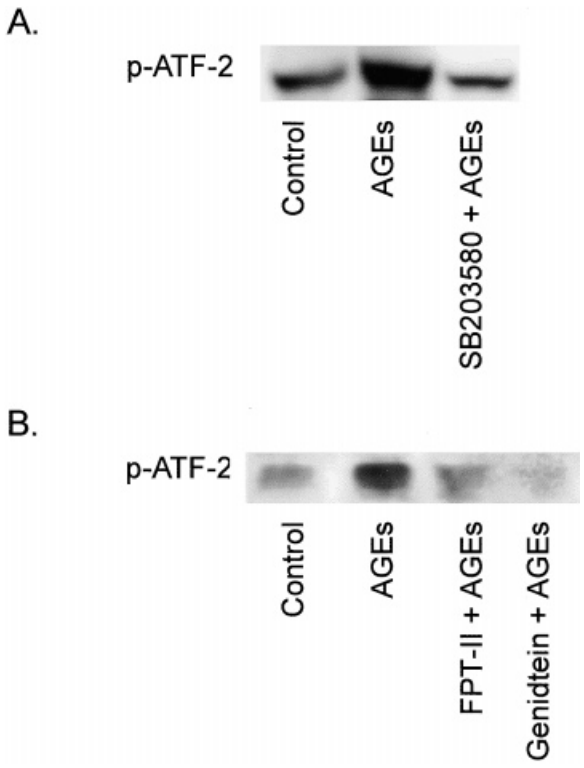

Fig. 7. Effects of SB203580, genistein and FPT inhibitor-II on AGEs-stimulated increase in p38 MAPK activity in C6 glioma cells. C6 glioma cells were pretreated with SB203580 (10 μM) (A), FPT inhibitor-II (20 μM) or genistein (20 μM) (B) for 30 min before the addition of 300 μg/ml BSA-AGEs for 1 h. After incubation, the cells were lysed, and the p38 MAPK activity was determined with an immunocomplex kinase assay using ATF-2 as the substrate as described in *Methods.*

LPS-stimulated iNOS expression is inhibited by the tyrosine kinase inhibitors in murine macrophages [24] and in retinal epithelial cells [25]. Inhibition of AGEs-stimulated iNOS expression and nitrite release by genistein, suggests that the responses are also mediated by signaling through tyrosine phosphorylation. In rat pulmonary artery smooth muscle cells, activation of the receptor of AGEs triggers a p21 Ras-dependent MAPK pathway regulated by oxidant stress [19]. In the present study, we demonstrated that the AGEs-induced iNOS expression and nitrite release were inhibited by Ras inhibitor, FPT inhibitor II, and p38 MAPK inhibitor, SB203580. These results suggest that the activation of Ras and p38 MAPK are critical in the induction of iNOS caused by AGEs. Furthermore, we found that AGEs induced increase in p38 MAPK activity in C6 glioma cells, and this effect was inhibited by genistein, FPT inhibitor-II, or SB 203580. These findings suggest that the activations of tyrosine kinase and Ras were the upstream signals of the AGEs-induced p38 MAPK activation. Additionally, we have found that AGEs induced iNOS expression and NO accumulation were inhibited by the PKC inhibitor, Ro 31-8220 and Go 6976, and the MEK inhibitor, PD98059 (unpublished observation), suggesting PKC and ERK may also be involved in the signal transduction pathways by which iNOS were induced.

Treatment of C6 glioma cells with AGEs results in a strong upregulation of iNOS protein. However, the AGEs-induced augmentation of nitrite accumulation remains only two-fold. This could be due to high basal level seen in C6 glioma cells. Indeed, we demonstrated that the consititutively expressed eNOS (but not nNOS) is presented in C6 glioma cells. The detailed mechanism by which iNOS expression is up-regulated is not totally clear. The murine iNOS promoter contains 24 transcriptional factor binding sites, including those for NF-κB, activator protein-1 (AP-1), activating transcription factor (ATF)/cAMP response element-binding protein (CREB), and the STAT family of transcription factors [26]. Some of these transcription factors are regulated by p38 MAPK [27]. It is possible that regulation of transcription initiation by p38 MAPK mediates AGEs-stimulated iNOS expression.

In conclusion, AGEs may activate the pathways of tyrosine kinase and Ras to induce p38 MAPK activation, which in turn induces iNOS expression and NO production in C6 glioma cells. Although the detailed signaling mechanisms remain unclear, distinct signaling pathways appear to be involved. Further work is required to elucidate whether other pathways are involved in mediating AGEs-mediated inflammation, which subsequently results in neuronal damage.

Acknowledgments

The work was supported by grants NSC-89-2320-B-038-009 and NSC89-2314-B-038-041 from the National Science Council, Taipei, Taiwan, R.O.C. The authors wish to thank Maan-Tzwu Chen and Shiau-Ren Leu for their skilled technical assistance.

References

1. Brownlee A, Vlassara H, Cerami A. Advanced glycosylation end products in tissue and the biochemical basis of diabetic complications. New England Journal of Medicine 1988; 318: 1315–21.

2. Brownlee M. Glycosylation products as toxic mediators of diabetic complications. Annual Review of Medicine 1991; 42: 159–66.
3. Smith M.A, Siedlak SL, Richey PL, Nagaraj RH, Elhammer A, Perry G. Quantitative solubilization and analysis of insoluble paired helical filaments from Alzheimer disease. Brain Research 1996; 717: 99–108.
4. Munch G. Thome J. Foley P. Schinzel R. Riederer P. Advanced glycosylation endproducts in aging and Alzheimer's disease. Brain Research Reviews 1997; 23: 134–43.
5. Schimidt AM, Weidman E, Lalla E, Tan SD, Hori O, Cao R, Brett J.G, Lamster TB Advanced glycation end products (AGEs) induced oxidant stress in the gingiva: a potential mechanism underlying accelerated periodontal disease associated with diabetes. Journal of Periodontal Research 1996; 31: 508–15.
6. Seftel AD, Vaziril ND, Ni Z, Ramjouei K, Fogarty J, Hampel N, Polak J, Wang RZ, Ferguson K, Block C, Haas C. Advanced glycation end products in human penis: elevation in diabetic tissue, site of deposition and possible effect through iNOS or eNOS. Urology 1997; 50: 1016–26.
7. Chibber R, Molinatti PA, Rosatto N, Lambourne B, Kohner EM. Toxic action of advanced glycation end products on cultured retinal capillary pericytes and endothelial cells: relevance to diabetic retinopathy. Diabetologia 1997; 40: 156–64
8. Abordo EA, Westwood ME, Thornalley PJ. Synthesis and secretion of tumor necrosis factor-alpha by mature human monocytes and human monocytic THP-1 cells induced by human serum albumin derivatives modified with methyglyoxal and glucose-derived advanced glycation endproducts. Immunology Letters 1997; 53: 7–13.
9. Rojas A, Caveda I, Romay C, Lopez E, Valdes S, Padron J, Glaria L, Martinez O, Delgado R. Effects of advanced glycosylation end products on the induction of nitric oxide synthase in murine macrophages. Biochemical and Biophysical Research Communication 1996; 225: 358–62.
10. Ramirez R, Bedoya FJ, Chiara MD, Sobrino F. Inhibitory effect of albumin-derived advanced glycation products on PMA-induced superoxide anion production by rat macrophages. Life Sciences 1997; 60: 2279–89.
11. Knowles RG, Moncada S. Nitric oxide synthases in mammals. Biochemical Journal 1994; 298: 249–58.
12. Gross SS, Wolin MS. Nitric oxide: pathophysiological mechanisms. Annual Review of Physiology 1995; 57: 737–69.
13. Li YM, Dickson DW. Enhanced binding of advanced glycation end products (AGEs) by the ApoE4 isoform links the mechanism of plague deposition in Alzheimer's disease. Neuroscience Letters 1997; 226: 155–58.
14. Zimmerman GA, Meistrell III M, Bloom O, Cockroft KM, Bianchi M, Risucci D, Broome J, Farmer P, Cerami A, Vlassara H, Tracey KJ. Neurotoxicity of advanced glycation endproducts during focal stroke and neuroprotective effects of aminoguanidine. Proceedings of the National Academy of Sciences of the United States of America 1995; 92: 3744–48.
15. Horie K, Miyata T, Yasuda T, Takeda A, Yasuda Y, Maeda K, Sobue G, Kunokawa K. Immunohistochemical localization of advanced glycation end products, pentosidine, and carboxymethyllysine in lipofuscin pigments of Alzheimer's disease and aged neurons. Biochemical and Biophysical Research Communication 1997; 236: 327–32.
16. Amore A, Cirina P, Mitola S, Peruzzi L, Gianolio B, Rabbone I, Sacchetti C, Cerutti F, Grillo C, Coppo R. Nonenzymatically glycated albumin (Amadori adducts) enhances nitric oxide synthase activity and gene expression in endothelial cells. Kidney International 1997; 51: 27–35.
17. Li YM, Mitsuhashi T, Wojciechowicz D, Shimizu N, Li J, Stitt A, He C, Banerjee D, Vlassara H. Molecular identity and cellular distribution of advanced glycation endproduct receptors: relationship of p60 to OST-48 and p90 to 80K-H membrane proteins. Proceedings of the National Academy of Sciences of the United States of America 1996; 93: 11047–52.
18. Higashi T, Sano H, Saishoji T, Ikeda K, Jinnouchi Y, Sanzaki T, Morisaki N, Raucala H, Schichiri M, Horiuchi S. The receptor for advanced glycation end products mediates the chemotaxis of rabbit smooth muscle cells. Diabetes 1997; 46: 464–72.
19. Lander HM, Rauras JM, Ogiste JS, Hori O, Moss RA, Schmidt AM. Activation of the receptor for advanced glycation end products triggers a p21 (ras)-dependent mitogen-activated protein kinase pathway regulated by oxidant stress. Journal of Biological Chemistry 1997; 272: 17810–14.
20. Satoh H, Togo M, Hara M, Miyata T, Han K, Maekawa H, Ohno M, Hashimoto Y, Kurokawa K, Wanatabe T. Advanced glycation end products stimulate mitogen activated protein kinase and proliferation in rabbit vascular smooth muscle cells. Biochemical and Biophysical Research Communication 1997; 239: 111–5.
21. Gross SS, Jaffe EA, Levi R, Kilbourn RG. Cytokine-activated endothelial cells express an isotype of nitric

oxide synthase which is tetrahydrobiopterin-dependent, calmodulin-independent and inhibited by arginine analogues with a rank order of potency characteristic of activated macrophages. Biochemical and Biophysical Research Communication 1991; 178: 823–9.
22. Wallace MN, Geddes JG, Farquhar DA, Masson MR. Nitric oxide synthase in reactive astrocytes adjacent to beta-amyloid plagues. Experimental Neurology 1997; 144: 266–72
23. Smith MA, Richey PL, Sayre LM, Beckman JS, Perry G. Widespread perxynitrite-mediated damage in Alzheimer's disease. Journal of Neuroscience 1997; 17: 2653–2657.
24. Dong Z, Qi X., Xie K, Fidler IJ. Protein tyrosine kinase inhibitors decrease induction of nitric oxide synthase activity in lipopolysaccharide-responsive and lipopolysaccharide-non-responsive murine macrophages. Journal of Immunology 1993; 151: 2717–24.
25. Faure V, Courtois Y, Goureau O. Tyrosine kinase inhibitors and antioxidants modulate NF-κB and NOS-II induction in retinal epithelial cells. American Journal of Physiology 1998; 275: C208–15.
26. Xie QW, Wishnan R and Nathan C. Promotor of the mouse gene encoding calcium-independent nitric oxide synthase confers inducibility by interferon γ and bacterial lipopolysaccharide. Journal of Experimental Medicine 1993; 177: 1779–84.
27. Karin M. Signal transduction from the cell surface to the nucleus through the phosphorylation of transcription factors. Current Opinion in Cell Biology 1994; 6: 415–24.